Available online at www.sciencedirect.com
ScienceDirect
Bioorganic Chemistry 34 (2006) 424–444
BIOORGANIC CHEMISTRY
www.elsevier.com/locate/bioorg

Structural and thermodynamic studies of simple aldose reductase–inhibitor complexes

June M. Brownlee [1], Erik Carlson [2], Amy C. Milne [3], Erika Pape [4], David H.T. Harrison [*,1]

Department of Biochemistry, Medical College of Wiscosin, Milwaukee, WI, USA

Received 8 August 2006

Abstract

The competitive inhibition constants of series of inhibitors related to phenylacetic acid against both wild-type and the doubly mutanted C298A/W219Y aldose reductase have been measured. Van't Hoff analysis shows that these acids bind with an enthalpy near −6.8 kcal/mol derived from the electrostatic interactions, while the 100-fold differences in binding affinity appear to be largely due to entropic factors that result from differences in conformational freedom in the unbound state. These temperature studies also point out the difference between substrate and inhibitor binding. X-ray crystallographic analysis of a few of these inhibitor complexes both confirms the importance of a previously described anion binding site and reveals the hydrophobic nature of the primary binding site and its general plasticity. Based on these results, *N*-glycylthiosuccinimides were synthesized to demonstrate their potential in studies that probe distal binding sites. Reduced α-lipoic acid, an anti-oxidant and therapeutic for diabetic complications, was shown to bind aldose reductase with a binding constant of 1 μM.

Keywords: Aldose reductase; Lipoic acid; ARI; van't Hoff; X-ray crystallography; Ligand binding

* Corresponding author.
E-mail address: David.Harrison@RosalindFranklin.edu (D.H.T. Harrison).
[1] Present address: Department of Biochemistry and Molecular Biology, Chicago Medical School, Rosalind Franklin University of Medicine and Science, North Chicago, IL 60064, USA.
[2] Present address: Department of Neuroscience, University of Minnesota, Minneapolis, MN 55455, USA.
[3] Present address: Department of Chemistry, Rosenstiel Basic Medical Sciences Research Center, Brandeis University, Waltham, MA 02453, USA.
[4] Present address: Wisconsin Department of Natural Resources, Milwaukee, WI, USA.

0045-2068/$ - see front matter
doi:10.1016/j.bioorg.2006.09.004

1. Introduction

Aldose reductase (EC 1.1.1.21, AKR1B1) is a ubiquitous member of the aldo-keto reductase superfamily with broad substrate specificity. Members of this superfamily catalyze the NADPH-dependent reduction of a variety of aldehydes and short-chain ketones to their corresponding alcohols. Aldose reductase catalyzes the first step in the polyol pathway (converting glucose to sorbitol), and has been implicated in diabetic complications in individuals with poorly controlled glucose levels, and as such this enzyme has been considered a therapeutic target and has been an active area of investigation for several decades [1–3]. In spite of this large effort in understanding the structure and mechanism of the enzyme, the seeming success of aldose reductase inhibitor (ARIs)[5] in numerous animal trials, and some positive outcomes in human clinical trials [5,6], no ARI yet has succeeded in becoming an FDA approved drug [1,4]. Many believe that the broad aldehyde substrate specificity range of aldose reductase combined with the fact that other aldo-keto reductases may be inhibited by an ARI has greatly complicated the development of successful drugs against this target and has made inhibitor specificity a real concern [7–9].

It is often assumed that a molecule that tightly binds to and inhibits an enzyme will have more specificity than one that binds weakly. However, the free energy of a ligand in solution can have as great an influence on the binding equilibrium (K_{eq}) as the free energy of the ligand in the context of the enzyme binding site. The enthalpic contribution to free energy (ΔH) can be correlated with the formation of specific interaction with the macromolecule, whereas entropic contributions to free energy ($-T\Delta S$) are often the result of aspects of the ligand's interaction with the solvent. The enthalpy of binding is often measured as the heat of binding at constant pressure by isothermal titration calorimetry (ITC). However, ITC experiments require that each macromolecule is functional, since the reliable fitting of ΔH and ΔG to the titration curve rely on knowing the stoichiometry of binding (particularly for weakly binding ligands). Aldose reductase proved to be too variable in the number of functional binding sites as purified from *Escherichia coli* to meet this requirement. To overcome this difficulty, the temperature dependence of the competitive inhibition constant was fit with the van't Hoff equation to derive the enthalpy of binding. Since, K_i is determined by only catalytically competent enzyme molecules and does not include contributions from secondary binding sites, van't Hoff analysis of K_i reports only the enthalpy of binding that is important for future inhibitor design. Since K_i is equal to K_d only for competitive inhibition, it was necessary to measure the kinetics for the oxidative reaction, where the ARIs studied inhibit competitively. Most ARIs give complex inhibition patterns in the reductive direction. In this manner, the free energy of inhibitor and substrate binding can be separated into their component enthalpic and entropic parts, ΔH and $-T\Delta S$. Additionally, this method allows the measurement of the temperature dependence of the turnover number (k_{cat}), from which the activation energy can be derived.

The catalytic mechanism of aldose reductase follows an ordered bi–bi mechanism, where the NADPH binds, followed by aldehyde binding, chemistry, alcohol release and lastly $NADP^+$ release [10]. Aldose reductase folds as an $(\alpha/\beta)_8$ barrel that has an additional two amino terminal β-strands that form the bottom of the barrel and an additional two

[5] *Abbreviations used:* ARI, aldose reductase inhibitor; NADP(H), reduced or oxidized nicotinamide adenosine dinucleotide phosphate; C298A/W219Y, the cysteine 298 to alanine and tryptophan 219 to tyrosine doubly mutated enzyme; ITC, isothermal titration calorimetry.

α-helices termed H1 and H2 that are found between the seventh β-strand and the seventh α-helix of the barrel and after the eighth α-helix of the barrel, respectively [11,12]. A $NADP^+$ cofactor lies in an extended conformation across the barrel, with its nicotinamide ring lying at the bottom of a large cavity near the top of the barrel to form the active site near Tyr 48, His 110, and Cys 298 [12]. In aldose reductase, the hydroxyl of tyrosine 48 protonates the oxygen atom of the substrate during catalysis[13]. In recognition of the specificity problem, a number of new approaches to ARI design have been used; these approaches combine sequence homology data and high resolution X-ray crystallographic data. X-ray and neutron diffraction structures are known to very high resolution for a number of tight binding, highly specific human aldose reductase-ARI complexes [14–19]. These studies reveals an anion binding site formed near the oxidized nucleotide substrate ($NADP^+$) at a point that is nearly equidistant (~2.8 Å) from the C4 carbon of the nicotinamide ring, the OH oxygen of tyrosine 48, and the Nε2 nitrogen of histidine 110 [20]. Consistent with mutagenesis data that shows that Trp 20 is import for inhibitor binding [21], the crystal structures of these bound inhibitors show that each inhibitor is in van der Waals contact with this tryptophan. However, the extent of this interaction varies amongst the known ARI structures. The ring system of Alrestatin is stacked on Trp 20, which allows a second Alrestatin molecule to stack on the first Alrestatin, and interact with the specificity determinant [19,22].

Lipoic acid has recently received a great deal of attention as a therapy for the diabetic complications of neuropathy, nephropathy and hyperglycemic cataracts. Approximately 15 clinical trials of various sizes and design have been completed, and this molecule is approved as a drug in Germany while it remains under study and available as a dietary supplement in the United States. Effective dosages for symptoms of neuropathy have been achieved at 600 mg i.v. or 1800 mg orally, per day [23]. The rationale generally cited behind administering high doses of this otherwise endogenously produced cofactor is the antioxidant potential of dihydrolipoic acid, the reduced form of the molecule [24]. However, the ability of dihydrolipoic acid to chelate metals has also been noted. Lipoic acid is efficiently absorbed and readily trafficked into the cytosol and the mitochondria, though it is unclear whether a specific transport system exists or whether movement across membranes is simply a result of the amphipathic nature of this molecule. Inside the cell, lipoic acid is readily converted between the oxidized and reduced species [25]. It is generally believed that oxidative stress is an important component of diabetic complications and that antioxidants will have a beneficial effect on patients.

Initially, we chose to study the structure activity relationships of phenylacetic acid substituted at various positions (Fig. 1). For a selected series of compounds, we examined both the enthalpy of binding (by making a van't Hoff plot of the temperature dependence of the inhibition constant) and the crystal structure. As a result of these measurements, we were also able to determine the activation energy of the enzyme and the enthalpy and entropy of benzyl alcohol binding. We went on to examine many of these compounds in the context of the doubly mutated C298A/W219Y enzyme that was used to determine the structure of the Alrestatin complex and is known to have a faster k_{cat} and larger K_m than the wild-type enzyme [19]. Our interest in aldose reductase ligand binding is to understand the fundamental thermodynamic forces that govern the binding of this particular pharmacophore so these principles can be incorporated into future designs. A simple series of *N*-glycylthiosuccinimides were synthesized to demonstrate the principles learned. Due to the surprising strength of hexanoic acid as an aldose reductase inhibitor (~65 μM),

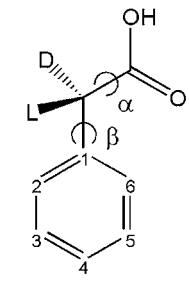

Phenylacetic acid
(D,L = OH for
d,l-mandelic acid)

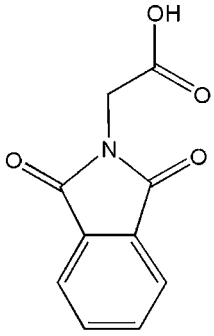

N-phthaloylglycine

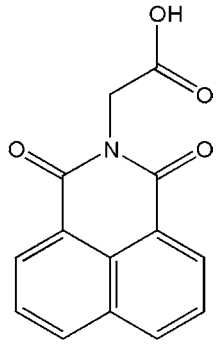

Alrestatin

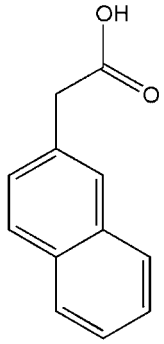

2-napthylacetic acid

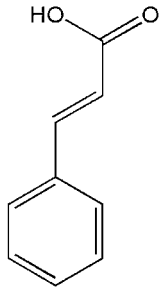

t-cinnamic acid

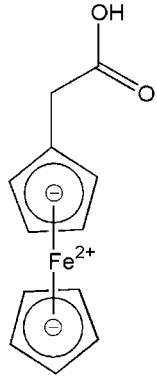

Ferrocene acetic acid

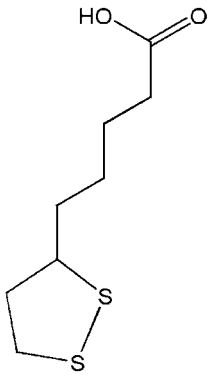

Lipoic Acid

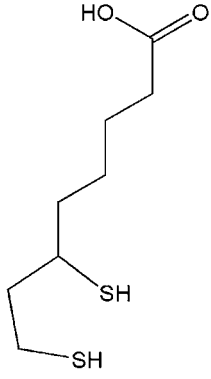

Dihydrolipoic Acid

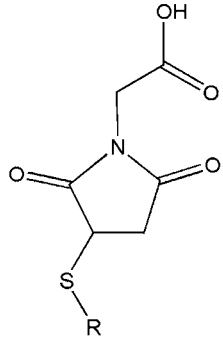

N-glycylthiosuccinimides

Fig. 1. The chemical structures of the acids examined in this study.

we postulated that the recently popular therapeutic for ameliorating diabetic complications, α-lipoic acid might also be an aldose reductase inhibitor, and it is, although the structure does not reveal how the thiols contribute to binding.

2. Materials and methods

2.1. Chemicals

All inhibitory acids were obtained from Aldrich, Milwaikee, WI, except 2-hydroxyphenylacetic acid which was obtained from Acros, Pittsburgh, PA. PEG6000 used in crystallization of aldose reductase was from Fluka, Switzerland. All other chemicals were from Fisher Scientific, Pittsburgh, PA, or Sigma Chemical, St. Louis, MO, and were of the highest quality available.

2.2. Protein purification

Aldose reductase protein and variants thereof were expressed in a pET vector in *E. coli* strain BL21(DE3) (Novagen, Madison, WI), and purified as previously described [38]. Protein eluted off the final chromatographic column was concentrated by ultrafiltration and stored in the chromatography buffer (5 mM sodium phosphate, 0.1 mM EDTA, and 7 mM mercaptoethanol, pH 7.7). Protein concentration was determined using the Bio-Rad assay and confirmed by specific activity measurements at 25 °C using 160 mM NADPH and 1.0 mM DL-glyceraldehyde as substrates, and the value of 0.83 μmol NADPH per min per 1 μg of enzyme ($M_W = 35{,}727$ kDa, $V/E_t = 0.5\ s^{-1}$.) Specific activity determinations as well as all other kinetic measurements were carried out in 0.10 M sodium phosphate buffer, pH 7.0.

2.3. Crystal growth and ligand binding

Crystals were grown at 4 °C by the hanging drop vapor diffusion method. As previously reported, the droplets were suspended over wells containing 20% (w/w) polyethylene glycol (PEG) 6000 and 50 mM sodium citrate, pH 5.0. The droplets contained equal volumes of "well" solution and the solution of aldose reductase protein in chromatography buffer (23–25 mg/mL). Into each droplet, one small "seed" crystal was introduced. Crystals grew to maximum size in approximately one month. Fully grown crystals were stabilized by a brief treatment with 0.1–1.0% glutaraldehyde, a cross-linking reagent. Inhibitory carboxylate molecules were then exchanged for citrate molecules in the active site via a series of successive soaks in PEG 6000 solutions with increasing concentrations of inhibitory molecules.

2.4. Data collection, processing and crystallographic refinement

Crystals were mounted in a thin-walled glass capillary tube, and diffraction data were collected at 4 °C on an *R*-axis IIC image plate detector system with a Rigaku RU200 rotating anode generator operating at 50 kV and 100 mA with a graphite monochromator. The detector distance was kept at 90 mm and each frame of data corresponded to either a 1° or 1.5° oscillation. The diffraction data were processed with the DENZO/SCALEPACK package [39], and the statistics are given in Table 1. Initial phases were calculated by

Table 1
X-ray crystallographic data

	Wild-type					C298A/W219Y	
	Phenylacetic acid	2-Hydroxyphenylacetic acid	Hexanoic acid	Lipoic acid	2,6-Dichlorophenylacetic acid	Phenylacetic acid	2,6-Dichlorophenylacetic acid
R_{merge} (%)	8.7	8.1	5.3	3.9	8.7	6.7	10.3
Completeness (all) (%)	93.3	99.0	89.2	79.4	81.2	85.2	93.6
6.0–2.5 Å (%)	96.0	99.5	91.3	87.5	97.7	92.4	99.2
Last shell (%)	71.3	97.1	82.0	53.6	57.3	70.9	70.7
Total reflections ($I/\sigma > 1$)	72,172	207,347	53,313	26,639	87,290	43,548	65,473
Unique reflections	23,338	23,020	20,674	17,234	28,352	18,241	20,062
Dimensions (Space Group: $P2_12_12_1$ $\alpha = \beta = \gamma = 90.0$)							
a (Å)	49.9	50.1	50.0	50.0	50.0	50.1	50.0
b (Å)	67.0	66.9	67.0	67.0	67.1	66.8	66.2
c (Å)	92.1	92.0	92.0	91.9	92.1	92.1	92.4
Refinement resolution (Å)	30.0–1.90	30.0–1.95	30.0–1.95	20.0–2.0	30.0–1.70	30.0–2.0	30.0–2.0
R (working)	0.174	0.228	0.190	0.193	0.195	0.209	0.218
R (free)	0.220	0.259	0.252	0.239	0.242	0.263	0.268
RMSD from ideal[a]							
Length (Å)	0.010	0.009	0.007	0.009	0.010	0.007	0.007
Angles (°)	1.144	1.117	1.322	1.095	1.198	1.308	1.269
Ramachandran (%)							
Most favored	91.3	89.9	91.3	91.3	91.3	90.9	92.1
Additionally	8.7	10.1	8.7	8.7	8.3	9.1	7.5
Generously	0.0	0.0	0.0	0.0	0.4	0.0	0.4
PDB accession ID	2INE	2INZ	2IQ0	2IQD	2IS7	2ISF	2IPW

[a] Engh and Huber [37].

X-PLOR [26] from the native structure with $NADP^+$ bound but without water or other ligands present. The initial electron density maps after rigid-body refinement were used to locate the positions of the inhibitory carboxylate species. Inhibitor molecules which were not available from the HIC-Up database [27] were built and the associated parameter files generated with the program INSIGHT (Accelrys, Inc., San Diego, CA) Inhibitor molecules were fit into the density using the program O [28]. Water molecules were added to the model manually and with the aid of the WATERPICK module of X-PLOR. The results after several rounds of manual model building and refinement are summarized in Table 1. Molecular graphics used in Figs. 5–7 were produced using PyMOL [40].

2.5. Steady state kinetic parameters

The production of NADPH from $NADP^+$ and benzyl alcohol or xylitol was monitored by an increase in NADPH fluorescence (ex: 340 nm; em: 460 nm) using an SLM-Aminco 4800C fluorometer and in 0.1 M phosphate buffer (pH 7.0). Fluorescence was calibrated versus a solution of either 45 or 4.5 μM NADPH which had been recently quantitated by UV–visible absorbance ($\varepsilon_{340} = 6200\ M^{-1}\ cm^{-1}$). The progress of the reaction was followed over an initial linear period of 1–5 min corresponding to less than 10% of the total reaction. Benzyl alcohol concentrations ranged from 0.25 to 16 mM, while xylitol concentrations ranged from 50 mM to 1 M, with the $NADP^+$ present at 45 μM ($K_m(NADP) < 2$ μM) and not varied and enzyme concentrations less than 3 μM. For each inhibitor, at least three different inhibitor concentrations that bracketed K_i from 0.5- to 4-fold were used to determine K_i. For any one inhibitor concentration, the initial velocities were measured in duplicate or triplicate for at least five different substrate concentrations bracketing the apparent K_m.

In the absence of any inhibitor, the kinetic parameters $K_{m(alcohol)}$ and k_{cat} were obtained by fitting the initial velocities to the Michaelis–Menton equation Eq. (1).

$$v = \frac{V_{Max}[S]}{K_m + [S]} \tag{1}$$

In the presence of a competitive inhibitor K_i was also determined by initial velocities to a competitive form of the Michaelis–Menton equation Eq. (2).

$$v = \frac{V_{Max}[S]}{K_m(1 + [I]/K_i) + [S]} \tag{2}$$

The Marquardt algorithm implemented by the software package GRAFIT 3.0 (Erithacus Software, Middlesex, UK.) was used to fit the parameters to the data using nonlinear least-squares analysis. The linearity of slope replots, i.e. of plots of $K_{m(apparent)}/V_{max}$ versus [I], was used to confirm the competitive model of inhibition.

2.6. Temperature dependence of K_i, k_{cat}

The behavior of K_m and k_{cat} versus temperature was established by van't Hoff analysis across a range of temperatures from 277 to 333 K. A competitive inhibition model was established for each of the inhibitors at 298 K and the competitive inhibition model was established for phenylacetic acid and dichlorophenylacetic acid over the temperature range from 277 to 303 K. At this stage, initial velocity data were collected at a single alcohol concentration (either $\sim K_m$ or $\sim 2K_m$) while temperatures and inhibitor concentrations were varied, such that a full range of temperatures could be studied in a single day. The initial

velocities at a single temperature and alcohol substrate concentration were fit by nonlinear least squares analysis to a competitive inhibition model, treating K_m as constant, thus yielding temperature-dependent values of k_{cat} and K_i. For van't Hoff analysis, the temperature-dependent data were fit to the equation $\ln K_i = -\Delta H/R(1/T) + C$. The free energy ($\Delta G = -RT \ln K_i$) at 298 K (25 °C) was computed from this line, and $T\Delta S$ was computed as $T\Delta S = \Delta H - \Delta G$. Similarly, for the Arrhenius analysis, the temperature-dependent data were fit to the equation $\ln k_{cat} = -E_A/RT + \ln A$.

2.7. Synthesis of N-glyclylmaleimide and preparation of N-glycylthiosuccinimides

20 mmol maleic anhydride (1.88 g) and glycine in slight molar excess (1.74 g) were allowed to react at room temperature in 25 ml of glacial acetic acid for 3 h. The precipitate was collected and washed with cold deionized water. The precipitate was then dissolved in 65 °C deionized water and recrystallized by cooling, yielding 1.03 g *N*-glycyl maleic acid (6 mmol). The resulting solid was dissolved in 200 ml toluene and refluxed with 1.22 g (10 mmol) triethylamine over a Dean-Stark trap for 1 h, rotary evaporated under reduce pressure, and allowed to dry overnight under vacuum. The solid was dissolved in 9 ml of 0.01 N HCl and extracted with ethyl acetate. The organic layer was rotary evaporated to remove the ethyl acetate and dried under vacuum for 72 h. After drying the final yield was 0.16 g of an off-white powder that had a melting temperature of 103–106 °C. The NMR spectra gave ^{1}H singlet peaks at 4.17 and 6.88 ppm.

The production of the *N*-glycylthiosuccinimides were made by mixing an equal molar amounts of the *N*-glyclylmaleimide (about 20 mg) with the thiol of interest in 10 mM phosphate (pH 7.0). The reaction was monitored by measuring the absorbance at 305 nm and by measuring the loss of free thiol using Ellman's reagent, and the reactions were complete after no more than 45 min. This solution was then used to inhibit the enzyme without further purification.

3. Results

3.1. Inhibition of wild-type and C298A/W219Y mutated human aldose reductase by phenylacetic acid derivatives

In general, the binding constants of inhibitors of aldose reductase are stronger in the wild-type enzyme than in the C298A/W219Y doubly mutated enzyme. The basic pharmacophore, phenylacetic acid, binds to the wild-type enzyme with an inhibition constant of 96 μM (Table 2). The addition of a hydroxyl substituent at the β-carbon of phenylacetic acid (mandelic acid) shows that this group at this position results in lower affinity binding and that there is a small degree of stereoselectivity at this position. With the C298A/W219Y doubly mutated enzyme, the inhibition constant is proportional to the size of the substituent at the *ortho* (or 2) position of the phenyl ring (Fig. 2). The inhibition constants for the wild-type enzyme are much more varied with these singly substituted phenylacetic acids. For example, 2-hydroxyphenylacetic acid has a nearly 10-fold tighter K_i than that of 2-bromophenylacetic acid. With the addition of a second substituent to the other *ortho*-position of the phenyl ring, there is again an improvement in the strength of K_i compared to the mono-substituted compounds. However, the trend with size is once again reversed between the wild-type and the doubly mutated enzyme.

Table 2
Competitive inhibition constants for wild-type, the C298A/W219Y doubly mutated, and the C298A mutated aldose reductase as the reaction proceeds from the alcohol to the aldehyde at a temperature of 25 °C

	Wild-type (μM)	C298A/W219Y (μM)[d]	C298A (μM)[d]
Alrestatin	2.0 ± 0.1[a]	7.5 ± 0.4[a]	
N-Phthaloylglycine	1.5 ± 0.3[b]		
Phenylacetic acid	96. ± 16[b]	360. ± 50[c]	303. ± 32[b]
L-Mandelic acid	621. ± 102[c]		
D-Mandelic acid	361. ± 27[c]		
2-Fluorophenylacetic acid	13. ± 2[b]	100. ± 10[c]	
o-Tolylacetic acid	80. ± 14[b]	62. ± 10[c]	
2-Chlorophenylacetic acid	38. ± 12[b]	42. ± 4[c]	
2-Bromophenylacetic acid	38. ± 7[b]	11. ± 2[c]	
2-Hydroxyphenylacetic acid	3.5 ± 0.4[b]	32 ± 3[c]	18.1 ± 0.1
4-Chlorophenylacetic acid	34.2 ± 2.4[b]	170. ± 20[c]	
2,6-Difluorophenylacetic acid	2.5 ± 0.1	12. ± 2[c]	
2,6-Dichlorophenylacetic acid	4.4 ± 0.9[b]	1.0 ± 0.1[c]	
t-Cinnamic acid	280. ± 20[c]	1390. ± 200[c]	
2-Napthylacetic acid	6.2 ± 0.4[c]	94. ± 20[c]	
Ferrocene acetic acid	37.7 ± 4[c]		
Hexanoic acid	68.6 ± 9.1[c]		
D,L-Lipoic acid	25.5 ± 4.5[c]		
D,L-Lipoamide	86. ± 17.2[c]		
D,L-Dihydrolipoic acid	0.95 ± 0.13[c]		
N-Glycylthiosuccinimides			
β-mercaptoethanol	8.1 ± 1.8[b]		
Cysteine	14.0 ± 2[b]		
N-Acetylcysteine	2.3 ± 0.2[b]		
Cysteine methyl ester	6.5 ± 0.4[b]		
Glutathione	3.8 ± 0.3[b]		

[a] Data from Harrison et al. [19] using xylitol as a substrate.
[b] Determined using benzyl alcohol as a substrate.
[c] Determined using xylitol as a substrate.
[d] Blank if not determined.

3.2. Inhibition of wild-type and C298A/W219Y mutated human aldose reductase by other small acids

The placement of an additional methenyl group between the carboxylate and the phenyl ring (*i.e. trans*-cinnamic acid) appears to significantly weaken binding by about the same fold in both the wild-type and doubly mutated enzymes. 2-Napthylacetic acid is a much tighter inhibitor in wild-type aldose reductase than in the doubly mutated enzyme. Ferrocene acetic acid binds with a slightly tighter binding constant than phenyl acetic acid. This is interesting because the pentadienide ring is smaller than a phenyl ring, and thus might be expected to bind less tightly. However, the structure of Alrestatin bound to the C298A/W219Y doubly mutated aldose reductase suggested that there is indeed room for two rings stacked upon each other, with the second ring interacting with Trp 111 [19].

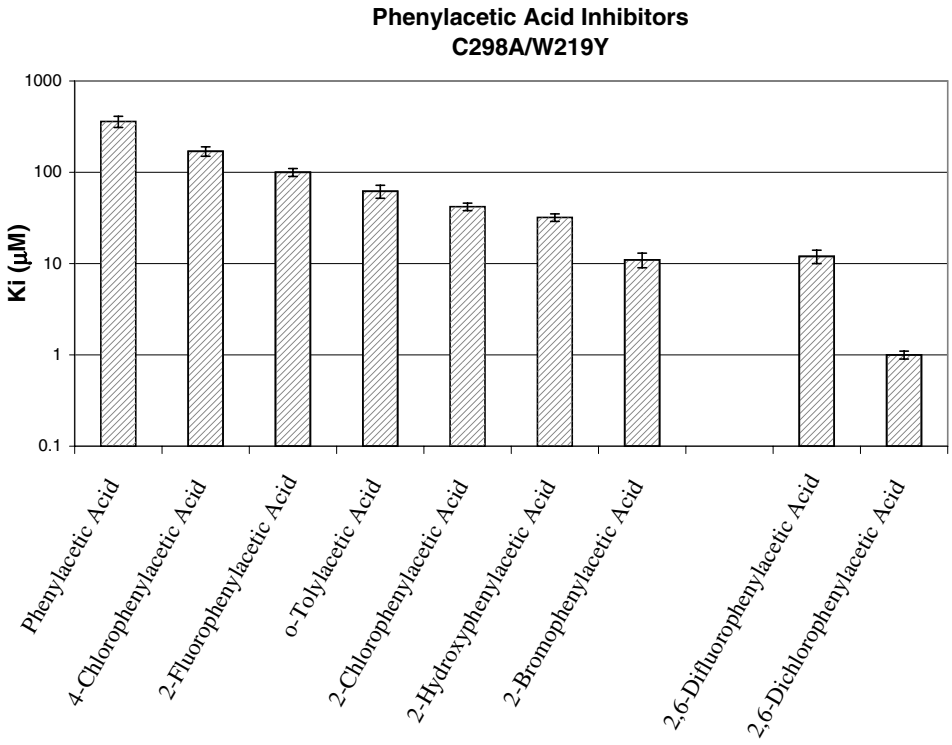

Fig. 2. Inhibition constants for a series of mono and di-substituted phenylacetic acid derivatives against the doubly mutated C298A/W219Y enzyme.

Hexanoic acid binds to the wild-type enzyme somewhat more tightly than the pharmacophore phenylacetic acid. This was unexpected, and suggested that the hydrophobic nature of the aldose reductase active site makes significant contributions to inhibitor binding rather than a reliance on pi-pi orbital interactions with Trp 20. The soluble eight carbon long molecule, D,L-lipoic acid, reported to be effective in the treatment of diabetic complications [29], binds to aldose reductase more tightly than hexanoic acid. Somewhat surprisingly, the reduced form of lipoic acid, D,L-dihydrolipoic acid, binds to wild-type aldose reductase tighter than any other molecule studied in this report. Interestingly, the uncharged molecule, D,L-lipoamide binds only 3-fold more weakly than D,L-lipoic acid. This must indicate that hydrogen bonding, hydrophobicity, and shape complementarity are more important for binding than simple charge-charge interactions.

3.3. Thermodynamic studies of inhibitors binding to human aldose reductase

The inhibition constants against the wild-type enzyme for the inhibitors phenylacetic acid, 2-chlorophenylacetic acid, and 2,6-dichlorophenylacetic acid show a nearly identical temperature dependence as indicated by slopes of the lines in the van't Hoff plot (Fig. 3). It is reasonable to deduce that the substituents on the phenyl ring are not contributing to the enthalpy of binding and that the negatively charged carboxylate interacting with the

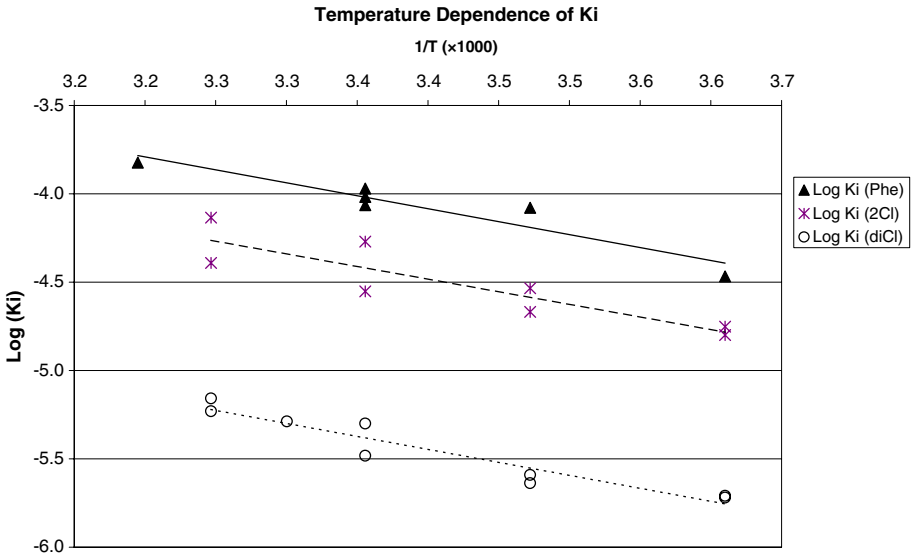

Fig. 3. A van't Hoff plot for the inhibitors phenylacetic acid (triangles), 2-chlorophenylacetic acid (asterisk), and 2,6-dichlorophenylacetic acid (circles). The near parallel lines indicate nearly identical enthalpies of binding.

positively charged nicotinamide ring is responsible for nearly all of the binding enthalpy. The negative entropy of binding for phenylacetic acid indicates that there are more states available to the system when phenylacetic acid and aldose reductase are free than when they are bound together.

Only 2-hydroxyphenylacetic acid has an enthalpy of binding that is significantly different from the average value of -7.0 ± 0.5 kcal/mol for the other compounds studied (Table 3, Fig. 4). To investigate the nature of the 2-hydroxyphenylacetic acid binding further, we "freshened" the aldose reductase by pre-incubating the enzyme in the presence of DTT for an hour at 37 °C prior to use, in order to completely reduce the cysteines of the enzyme, as

Table 3
Thermodynamic values for inhibitor binding to aldose reductase at a temperature of 25 °C

	ΔG (kcal/mol)	ΔH (kcal/mol)	$T\Delta S$ (kcal/mol)	R^2	df[a]
Phenylacetic acid	-5.5 ± 0.1	-6.7 ± 1.1	-1.2 ± 1.2	0.90	4
o-Tolylacetic acid	-5.6 ± 0.1	-6.3 ± 1.0	-0.8 ± 1.1	0.88	6
2-Chlorophenylacetic acid	-6.0 ± 0.2	-6.5 ± 1.4	-0.5 ± 1.6	0.78	6
2,6-Dichlorophenylacetic acid	-7.3 ± 0.1	-6.9 ± 0.6	0.4 ± 0.7	0.93	11
2,6-Dichlorophenylacetic acid[b]	-7.8 ± 0.1	-6.9 ± 1.4	0.9 ± 1.5	0.86	4
2-Hydroxyphenylacetic acid	-7.4 ± 0.1	-8.9 ± 0.7	-1.5 ± 0.8	0.91	14
2-Hydroxyphenylacetic acid[b]	-7.6 ± 0.1	*-7.1 ± 1.2*	0.5 ± 1.3	0.85	6
2-Hydroxyphenylacetic acid[c]	-6.5 ± 0.1	-7.6 ± 0.6	-1.1 ± 0.8	0.99	2
Hexanoic acid	-5.7 ± 0.1	-7.1 ± 0.9	-1.5 ± 1.0	0.96	3
N-Phthaloylglycine	-7.9 ± 0.1	-7.8 ± 0.7	0.1 ± 0.8	0.93	10

[a] Degrees of freedom in the fit to the line $\ln K_i = -\Delta H/R(1/T) + C$.
[b] Results after "freshening" the aldose reductase using the method of Ramana et al. [30].
[c] Results from C298A mutated enzyme.

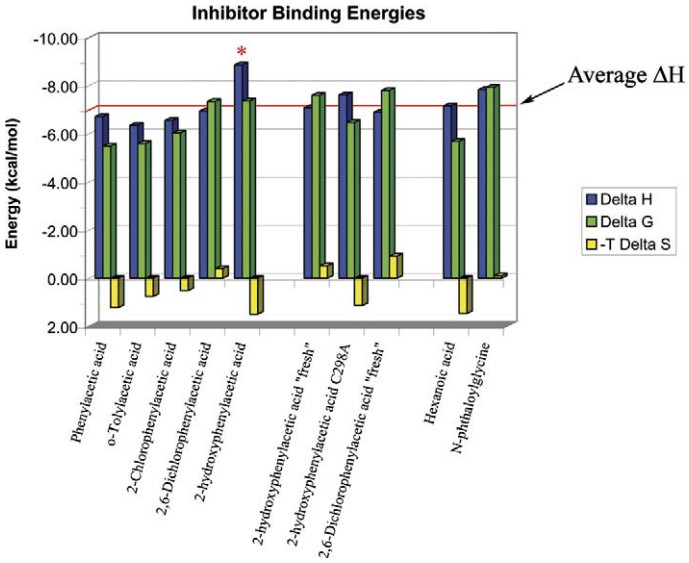

Fig. 4. Energies of inhibitor binding to wild-type aldose reductase: enthalpy (blue), free energy (green), entropic energy (yellow). The red line corresponds to the average enthalpy of binding (−7.0 kcal/mol) for all of the inhibitors excluding the "not freshened" 2-hydroxyphenylacetic acid. (For interpretation of the references to color in this figure legend, the reader is referred to the web version of this paper.)

described by Ramana et al. [30]. The "freshened" the aldose reductase resulted in a tighter free energy of binding (−7.6 kcal/mol), a weaker enthalpy of binding (−7.1 kcal/mol), and an entropy of binding that was slightly positive. To investigate further, we examined the thermodynamics of binding 2-hydroxyphenylacetic acid to the C298A mutated enzyme. The somewhat confusing results from this study showed a larger than average enthalpy of binding (−7.6 kcal/mol), and a negative entropy of binding. Our studies of 2,6-dichlorophenylacetic acid with both the normal and "freshened" enzyme suggest that the enthalpy of binding is generally unchanged.

The kinetics for benzyl alcohol oxidation by the aldose reductase at a temperature of 25 °C show Michaelis constants of 3.9 mM and 10.6 mM and turnover numbers of 0.051 and 0.213 s^{-1} for the wild-type and C298A mutated enzymes, respectively. The temperature dependence of the K_m for the alcohol substrate was measured while investigating the temperature dependence of the inhibition constants of the compounds studied in Table 4. It has been shown that the K_m for the alcohol substrate is good estimate for K_d [10]. Entropy is the driving force for benzyl alcohol association in both the wild-type and the C298A mutated enzyme (Table 4). This is consistent for a non-specific enzyme that will catalyze the oxidation and reduction of a broad array of substrates. The positive enthalpy of binding may suggest the displacement of some tightly bound water molecules from the active site prior to substrate binding. The wild-type enzyme shows a relatively large activation energy (17.9 kcal/mol) that is somewhat reduced in the C298A mutated enzyme (15.8 kcal/mol, p-value = 0.034). It has been hypothesized that a sulfur-aromatic bond is formed between Cys 298 and Trp 219 that stabilizes the closed form of the enzyme and limits the rate of catalysis in the direction of aldehyde reduction [10,31]. Both the

Table 4
Thermodynamic values for aldose reductase at a temperature of 25 °C

	K_m (mM)	ΔG (kcal/mol)	ΔH (kcal/mol)	$T\Delta S$ (kcal/mol)	R^2	df[a]
Benzyl alcohol (wild-type)	3.9 ± 0.9	-3.3 ± 0.1	1.6 ± 0.9	4.9 ± 1.0	0.25	9
Benzyl alcohol (C298A)	10.6 ± 1.1	-2.7 ± 0.1	1.9 ± 0.7	4.5 ± 0.8	0.76	2
		k_{cat} (s^{-1}) at 25 °C	Activation energy	Arrhenius constant		
Wild-type		0.05	17.9 ± 0.3	6.4×10^{11}	0.98	66
C298A		0.21	15.8 ± 0.4	8.6×10^{10}	1.00	2

[a] Degrees of freedom in the fit to the line $\ln k_{cat} = -E_A/RT + \ln A$ or the line $\ln K_m = -\Delta H/R(1/T) + C$.

differences in k_{cat} (4-fold) and activation energies seen here (at pH 7.0) are consistent with a conformational change that is the rate-limiting step in the wild-type enzyme, but is not the rate limiting step in the C298A mutated enzyme. This is different than what was inferred from rapid kinetics using the xylitol substrate at pH 8.0, where chemistry in the oxidative direction was 85% rate limiting [10]. The differences between this work and the earlier work [10,31] may be explained by the differences in substrates and pHs used in these two experiments.

3.4. Structural features found in inhibitor–aldose reductase complexes

To gain greater understanding of the differences in binding for these related compounds, a select subset of compounds including phenylacetic acid, 2-hydroxyphenylacetic acid, 2,6-dichlorophenylacetic acid, hexanoic acid, and lipoic acid were soaked into citrate containing human aldose reductase crystals and the X-ray structure of the complexes were determined to a high resolution limit of between 1.7 and 2.0 Å. Additionally, both phenylacetic acid and 2,6-dichlorophenylacetic acid were soaked into citrate containing C298A/W219Y doubly mutated aldose reductase crystals and the X-ray structure of the complexes were also determined. A least squares fit to all of these structures was performed to superimpose the coordinates of the ligands onto the active site. As expected, for each enzyme–inhibitor complex, the carboxylates bound in the $NADP^+$/Tyr48/His110 anion binding site. However, an unanticipated observation for the phenylacetic acid class of inhibitors was the fact that the aromatic rings did not pi stack onto Trp20 (Fig. 5B), as had previously been observed with Alrestatin. In fact, no two inhibitors position the ring in the exact same location (Fig. 5A), suggesting a degree of conformational flexibility in binding may be possible for phenylacetic acid. Relative to phenylacetic acid, the torsion angle between the ring and the β-carbon changes by 25° and 20° in 2-hydroxyphenylacetic acid and 2,6-dichlorophenylacetic acid, respectively. Additionally, the torsion angle between the carboxylate and the β-carbon changes by 45° in 2,6-dichlorophenylacetic acid, which gives rise to a 0.8 Å displacement of the sulfur atom of Cys 298 (Fig. 5A). The displacements associated with 2,6-dichlorophenylacetic acid complex suggest a degree of strain on the system.

In the doubly mutated enzyme crystal structure, in a rigid body manner the 2,6-dichlorophenylacetic acid rotates in the active site about 10° relative to its wild-type position (Fig. 6). This rotation results from the inhibitor in the doubly mutated enzyme relaxing into the area once occupied by the sulfur of Cys 298 (Positioning the 2-chloro 2.3 Å

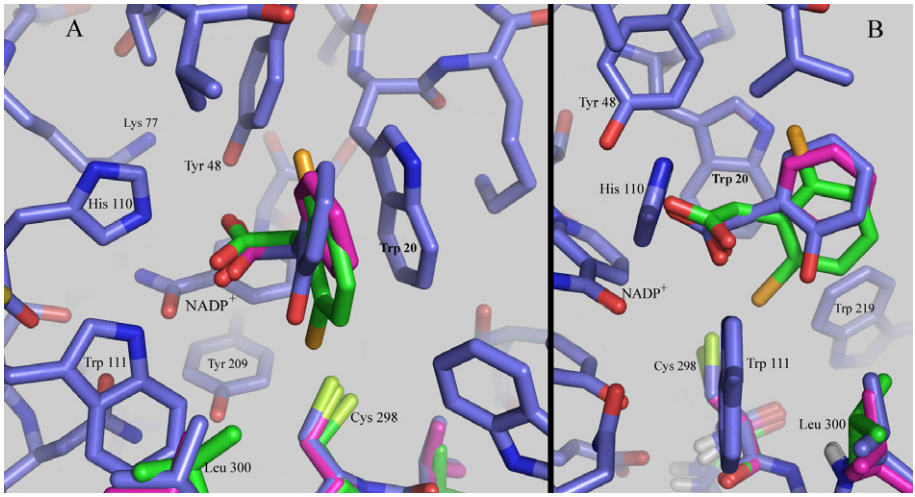

Fig. 5. (A) The superimposition of structures of the wild-type active site bound to phenylacetic acid (magenta [dark] carbons), 2-hydroxyphenylacetic acid (blue [medium] carbons), and 2,6-dichlorophenylacetic acid (green [light] carbons). Each inhibitor adopts its own conformation and positions its ring differently in the active site. The 2,6-dichlorophenylacetic acid displaces the sulfur atom of Cys 298 by 0.8 Å relative to the phenylacetic acid complex. (B) The same structures viewed from 90° away show that none of the inhibitors stack on the Trp 20 ring system.

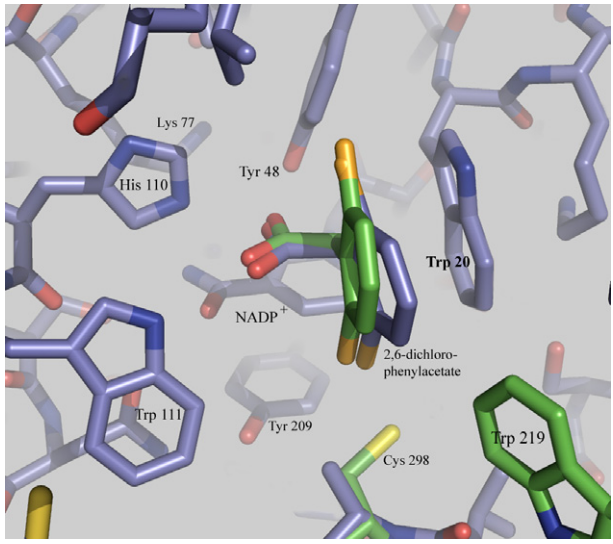

Fig. 6. The structures of 2,6-dichlorophenylacetic acid bound to the active sites of the wild-type (green [light] carbons) and the C298A/W219Y mutated enzyme (blue [dark] carbons). (For interpretation of the references to color in this figure legend, the reader is referred to the web version of this paper.)

from the position formerly occupied by the sulfur of Cys 298 rather than the 3.6 Å observed in the inhibitor-wild type complex). Further, the side chain of tyrosine 219 is disordered. In the phenylacetic acid C298A/W219Y mutated enzyme complex (structure not

shown), the phenylacetic acid does not change positions significantly relative to its position in the wild-type enzyme. Unlike either the previously described Alrestatin complex or the 2,6-dichlorophenylacetic acid structures, Tyr 219 uses the same $\chi 1$ torsion angle as Trp 219 of the wild-type enzyme.

The aliphatic inhibitors, hexanoic and α-lipoic acid, also utilized the canonical anion binding site and showed relatively elongated conformers of the aliphatic chain (Fig. 7). In the case of α-lipoic acid no electron density was observed after the sixth carbon indicating static or dynamic disorder of this end of the bound inhibitor molecule. Consequently, the position of the sulfur atoms was not defined. The structure of dihydrolipoic acid (reduced α-lipoic) would be of interest since it binds ~25-fold more tightly, but ligand oxidation during soaking would have prevented obtaining this structure and co-crystallization attempts failed.

3.5. Inhibition studies of human aldose reductase by N-glycylthiosuccinimides

Based on the improvement of the 2,6-dichloro phenylacetic acid relative to phenylacetic acid in inhibiting aldose reductase, a molecular platform that could be easily constructed was considered. *N*-Glyclylmaleimide was synthesized from maleic anhydride and glycine (see Section 2.7). To this compound, a few simple thiol containing compounds were added to demonstrate that the *N*-glycylthiosuccinimides could indeed bind aldose reductase with reasonable affinity. Both the β-mercaptoehanol adduct and the glutathione adduct demonstrate that the platform is capable of using a wide variety of substituents to probe the

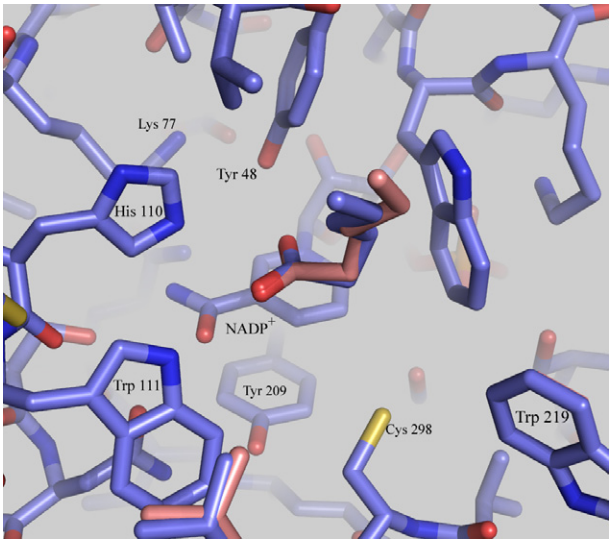

Fig. 7. The structures of hexanoic acid (blue [dark] carbons) and lipoic acid (salmon [light] carbons) bound to the active site of wild-type aldose reductase superimposed on each other. Both aliphatic chains make van der Waals contact with Trp 20. After following nearly the same path as hexanoic acid, the lipoic acid becomes disordered after the sixth carbon, consistent with an entropic rather than enthalpic basis for its tighter binding. (For interpretation of the references to color in this figure legend, the reader is referred to the web version of this paper.)

active site of an aldo-keto reductase, and yielded inhibition constants of 8.1 and 3.8 μM, respectively. The series of cysteine adducts demonstrate that additional charge near the glycyl carboxylate is not well tolerated, but that a single negative charge is preferred over a single positive charge.

4. Discussion

The Alrestatin class of ARIs can be thought of as a carboxylate β to a planar ring system. These inhibitors display uncompetitive or noncompetitive inhibition kinetics for the forward reaction catalyzed by aldose reductase (aldehyde to alcohol). Consistent with aldose reductase's ordered bi–bi mechanism, these inhibitors are competitive in the backwards reaction (alcohol to aldehyde). Since, the competitive inhibition constant is equal to the binding constant, studying these inhibitors is most informative utilizing the backwards reaction. The simplest commercially available member of this class of compounds is phenylacetic acid. Individual members of this class of compounds use different ring sizes and have different substituents (in addition to the acetic acid moiety). In addition, the temperature dependence of inhibition has been determined for selected inhibitors. The conformation and location of some of these inhibitors was determined using X-ray crystallography.

4.1. The effect of the carboxylate and substituents at the 2 and 6 positions on aldose reductase binding

Phenylacetic acid binds aldose reductase nearly 50-fold less tightly than Alrestatin, while the slightly more complex molecule 2,6-dichlorophenylacetic acid binds the wild-type enzyme 2-fold less tightly and the double mutant C298A/W219Y 7-fold more tightly than Alrestatin (Table 2). The thermodynamic studies show that these two inhibitors have nearly identical binding enthalpies as determined by van't Hoff analysis of the temperature dependence of inhibitor binding. Similar enthalpic contributions were also seen for the distantly related compound hexanoic acid. Combined, these data suggest that the main contribution to the binding enthalpy is the carboxylate moiety, which binds near the positively charged nicotinamide ring of $NADP^+$. It is also clear that the role of the two chlorine atoms of 2,6-dichlorophenylacetic acid is to reduce the entropy of the compound in solution relative to the entropy available to phenylacetic acid. The additional buried surface area contributed by the two additional chlorine atoms is too small for this entropy difference to be attributed to the "hydrophobic effect." Thus, the change in the entropy of binding can be thought of in terms of restricting the rotational freedom about the β torsion angle when the molecule is free in solution. Since both phenylacetic acid and 2,6-dichlorophenylacetic acid have nearly the same (restricted) conformational freedom when bound to the active site, the number of conformations available when free in solution must be different. Indeed molecular dynamic simulations suggest that the frequency with which the carboxylate moves from one side of the ring to the other is indeed limited in the dichloro compound. Thus, we hypothesize that limitation in conformational freedom in solution and the corresponding increase in ΔS is the result of restricting rotation about the β torsion angle. The observation that the size of the substituent at the 2 position appears to be the biggest factor in determining the K_i of phenylacetic acid derivatives for the C298A/W219Y doubly mutated enzyme is consistent with this hypothesis. The expanded size of the active site of the doubly mutated enzyme relative to the wild-type enzyme reduces

the amount of steric constrictions and additional hydrogen bonding possibilities and allows these trends to be observed without complication.

Since the enthalpic energy of binding is related to the breaking and making of non-covalent bonds (e.g. ionic bonds, hydrogen bonds, and dipolar [and induced dipolar] bonds), differences in enthalpy are likely to be due to differences in the bound complex. Conversely, in biological systems, entropic energies derive from the change in the number of states that the system can have when the ligand and macromolecule are free versus when the macromolecule and ligand form a complex. One large source of entropic energy is imbedded in the hydrophobic effect, the burying of the hydrophobic surface areas of ligand and macromolecule and the associated release of ordered solvent molecules; differences in this form of entropic energy between two ligands can be due to differences in how they bind in the complex, but can also be largely due to changes in the overall hydrophobicity of the ligand. Changes in conformational freedom of the ligand and macromolecule in the bound and free states represents another source of entropic energy. Since the bound state is conformationally limited, this form of entropic energy is largely due to limitations in the conformational entropy of the free state. Thus, changes to a ligands architecture that lead to net gains in binding entropy of this kind does not lead to increases in specificity, since it is the free state of the ligand that is determining the entropy of binding. For these reasons, others have postulated that antibiotic inhibitors that utilize enthalpic interactions with active site residues as the primary source of their binding energy are less susceptible to the development of resistant strains [32,33].

4.2. What could be the cause of the increased binding enthalpy for the 2-hydroxyphenylacetic acid?

A favorable interaction between the 2-hydroxyl group 2-hydroxyphenylacetic acid and Cys 298 is suggested by the difference in the inhibition constants for the wild-type and C298A/W219Y double mutant enzymes. The crystal structure of 2-hydroxyphenylacetic acid bound to the wild-type enzyme shows that the hydroxyl group is on the same side of the phenyl ring as the Cys 298 residue, although the sulfur–oxygen distance of 4.7 Å is too large to make a "hydrogen bond." Molecular dynamics simulations of 2-hydroxyphenylacetic acid *in vacuo* suggest that the hydrogen bond that forms between the carboxylate moiety and the hydroxyl moiety lowers the energy barrier to rotation about the β torsion angle relative to that which is observed in other ortho substituted molecules. Consistent with this calculation, the observed entropic energies ($-T\Delta S$) of binding for this inhibitor are 1.5 and 1.1 kcal/mol for the wild-type and C298A mutated enzyme, respectively (Table 3). The difference in the change in binding enthalpy ($\Delta\Delta H$) for this inhibitor between the wild-type and C298A mutated enzyme is considerable (1.8 kcal/mol). However, the enthalpy of binding to the C298A mutated enzyme is still greater than the average enthalpy of binding of the other phenylacetic acid derivative to the wild-type enzyme.

Since the change in enthalpy could be due to differences in oxidation for the wild-type and mutated enzymes, we tried "freshening" the enzyme prior to the thermodynamic studies. The van't Hoff plot showed a great deal of scatter, and as described above, the free energy of binding using the "freshened" enzyme is somewhat inconsistent with the other measurements, although the enthalpy is in line with the enthalpies seen with the other inhibitors. However, these results suggest the possibility that the

increased enthalpy originally seen for 2-hydroxyphenylacetic acid binding to the wild-type enzyme is due to the presence of sulfenic or sulfinic acid at Cys 298. Infrequently, in some our X-ray crystallographic studies of aldose reductase, we have seen electron density suggestive of sulfenic acid at Cys 298. It is possible to form an enthalpically favorable hydrogen bond with the hydroxyl group of 2-hydroxyphenylacetic acid. To substantiate that the thermodynamic studies of the other inhibitors tested remain valid, the energies of binding for 2,6-dichlorophenylacetic acid were determined with both the "freshened" and normally prepared enzyme. It was found that the enthalpy is unchanged while the free energy was somewhat improved after "freshening." It is worth noting that there is some evidence that C298 is specifically oxidized *in vivo* by nitric oxide and other compounds, which further complicates the process of inhibitor design [34,35].

4.3. Other ways in which the double mutation C298A/W219Y effects inhibitor binding

The improvement in K_i for 2,6-dichlorophenylacetic acid in the mutant enzyme can be understood in terms of steric conflicts between the 2-chloro moiety and the cysteine sulfhydryl moiety in the wild-type enzyme as seen in the crystal structures. This inhibitor is tightly packed into the active site pocket in both enzymes. However, the larger binding pocket in the mutant enzyme has detrimental effects on Alrestatin, phenylacetic acid, *t*-cinnamic acid, and 2-napthylacetic acid binding, although little effect on *o*-tolylacetic acid or 2-chlorophenylacetic acid. It is possible that the lack of a tryptophan residue in the double mutant reduces the "hydrophobic" contributions to binding these ring structures, while the lack of the cysteine sulfhydryl creates a new pocket for the chloro or methyl moieties to bind.

4.4. Differences between substrates and carboxylate inhibitors

Phenylacetic acid and benzyl alcohol share a number of common features with regards to size, aromaticity, and hydrophobicity and thus might be expected to interact with the enzyme in a similar manner. The enthalpy of binding for the substrate and that of the carboxylate inhibitors differ by about 8.3 kcal/mol in favor of the inhibitors. On the other hand, the entropic energy of binding for the substrate and that of the average inhibitor differ by about 5.4 kcal/mol in favor of the substrate. What is important about these two comparisons is that they show that the mode of binding in these two classes of compounds is fundamentally different. It must be realized that the K_m reflects the K_d for binding the substrate in a productive complex, while the K_i reflects the K_d for binding the inhibitor in the active site. The likely ionization state of the residues in the active site prior to binding both classes of the compounds can be assessed to yield a possible explanation for the fundamental difference in the partition of binding energies. In the case of the substrate binding to the enzyme, there is no electrostatic attraction between the positive charge on the nicotinamide ring and substrate hydroxyl group, although this hydroxyl group probably accepts a hydrogen bond from His 110 [13]. Further, the hydroxyl of Tyr 48 must be deprotonated, and initially withdrawn from the hydroxyl binding site by making a salt-bridge with the buried Lys 77, in order to form a Michaelis complex. The negative charge on Tyr 48 that is necessary for catalysis is not compatible with highly enthalpic carboxylate binding. To explain the unfavorable enthalpy of binding, we postulate that there is a

tightly bound water molecule at the hydroxyl position that must be displaced upon substrate binding at a large cost in enthalpy. On the other hand, when the carboxylate inhibitor binds, the positive charge on the nicotinamide ring should attract the negatively charged carboxylate. Further, the hydroxyl of Tyr 48 is protonated, as is the epsilon nitrogen of His 110, both of which can act as hydrogen bond donors. This configuration gives rise to the so-called "anion binding site." A postulated water molecule at the carboxylate oxygen position will be less tightly bound and less ordered when Tyr 48 is neutral in charge and will be displaced by the carboxylate at a lower enthalpy cost. Thus the differences in the energies of binding between the alcohol substrate and this class of inhibitors suggests that the carboxylate inhibitors bind an ionization state of the enzyme that is off the catalytic pathway.

4.5. α-Lipoic acid binding

The connection between AR and lipoic acid has not generally been made. Only in a couple of studies have attempts been made to examine AR activity in tissue samples subsequent to lipoic acid administration. In both studies rat lenses were used. In the first study, lipoic acid reduced enzymatic activity from 50 to 75% but this effect was attributed to metal chelation which was said to have impaired AR activation [34]. In the second study, lenses from rats fed a high-energy high starch diet and lipoic acid had lenses with 50% less AR activity, while lenses from rats fed a medium-energy diet and lipoic acid showed slightly increased AR activity levels. To our knowledge, no study of potential biochemical interactions of AR and lipoic acid has been undertaken in a purified, *in vitro* system. We report here that lipoic acid and especially dihydrolipoic acid can act simply as aldose reductase inhibitors, binding to the enzymic active site, and we attempt some preliminary characterizations of this interaction. We posit that this interaction constitutes another mechanism by which lipoic acid achieves its clinical efficacy.

5. Conclusion

The pharmacophore phenylacetic acid proved to bind to aldose reductase with essentially the same enthalpy of binding, without regard for the number or type of substituents. The differences in free energy amongst this class of inhibitors (~2 kcal/mol) were largely due to differences in the conformational freedom of the inhibitor free in solution rather than due to anything that might influence specificity. Trp 20 has been suggested to be an important inhibitor binding determinant [21,36]. Here, we show that its importance lies in its ability to make hydrophobic interactions with the carbon β to the carboxylate rather than making π–π stacking interactions, since none of the phenylacetic acid structures show evidence of π–π stacking (unlike the Alrestatin and zopoleresat structures [19,36]). Further, both lipoic acid and hexanoic acid show that they make van der Waals contact with Trp 20. The oxidation state of aldose reductase *in vivo* could prove to be a serious obstacle to designing inhibitors that have pharmaceutical efficacy. As a result of this investigation, it is shown that the easily synthesized compound, *N*-glyclylmaleimide, can make a stable platform for attaching a variety (library) of thiol containing compounds to further probe new specificity determinants. The finding that α-lipoic acid is an inhibitor of aldose reductase may suggest why it has clinical efficacy beyond that of other anti-oxidants.

Acknowledgments

Dedicated, with love, to the memory of Miriam "Mimi" Hasson, friend, ally, and colleague. I think she would have appreciated the minimalist approach to understanding inhibitor design and the integration of the different techniques used in this work. We also acknowledge the National Institutes of Health, DK-51697 for funding this work.

References

[1] L. Costantino, G. Rastelli, P. Vianello, G. Cignarella, D. Barlocco, Med. Res. Rev. 19 (1999) 3–23.
[2] K.H. Gabbay, Annu. Rev. Med. 26 (1975) 521–536.
[3] N. Hotta, Nagoya J. Med. Sci. 60 (1997) 89–100.
[4] M.A. Pfeifer, M.P. Schumer, D.A. Gelber, Diabetes 46 (Suppl. 2) (1997) S82–S89.
[5] N. Hotta, Y. Akanuma, R. Kawamori, K. Matsuoka, Y. Oka, M. Shichiri, T. Toyota, M. Nakashima, I. Yoshimura, N. Sakamoto, Y. Shigeta, Diabetes Care 29 (2006) 1538–1544.
[6] N. Hotta, T. Toyota, K. Matsuoka, Y. Shigeta, R. Kikkawa, T. Kaneko, A. Takahashi, K. Sugimura, Y. Koike, J. Ishii, N. Sakamoto, Diabetes Care 24 (2001) 1776–1782.
[7] J.M. Jez, M.J. Bennett, B.P. Schlegel, M. Lewis, T.M. Penning, Biochem. J. 326 (1997) 625–636.
[8] O.A. Barski, K.H. Gabbay, K.M. Bohren, Biochemistry 35 (1996) 14276–14280.
[9] K.M. Bohren, C.E. Grimshaw, K.H. Gabbay, J. Biol. Chem. 267 (1992) 20965–20970.
[10] C.E. Grimshaw, K.M. Bohren, C.J. Lai, K.H. Gabbay, Biochemistry 34 (1995) 4356–4365.
[11] J.M. Rondeau, F. Tete-Favier, A. Podjarny, J.M. Reymann, P. Barth, J.F. Biellmann, D. Moras, Nature 355 (1992) 469–472.
[12] D.K. Wilson, K.M. Bohren, K.H. Gabbay, F.A. Quiocho, Science 257 (1992) 81–84.
[13] K.M. Bohren, C.E. Grimshaw, C.J. Lai, D.H. Harrison, D. Ringe, G.A. Petsko, K.H. Gabbay, Biochemistry 33 (1994) 2021–2032.
[14] O. el-Kabbani, C. Darmanin, T.R. Schneider, I. Hazemann, F. Ruiz, M. Oka, A. Joachimiak, C. Schulze-Briese, T. Tomizaki, A. Mitschler, A. Podjarny, Proteins 55 (2004) 805–813.
[15] E.I. Howard, R. Sanishvili, R.E. Cachau, A. Mitschler, B. Chevrier, P. Barth, V. Lamour, Z.M. Van, E. Sibley, C. Bon, D. Moras, T.R. Schneider, A. Joachimiak, A. Podjarny, Proteins 55 (2004) 792–804.
[16] F. Ruiz, I. Hazemann, A. Mitschler, A. Joachimiak, T. Schneider, M. Karplus, A. Podjarny, Acta Crystallogr. D. Biol. Crystallogr. 60 (2004) 1347–1354.
[17] H. Steuber, M. Zentgraf, A. Podjarny, A. Heine, G. Klebe, J. Mol. Biol. 356 (2006) 45–56.
[18] M.P. Blakeley, A. Mitschler, I. Hazemann, F. Meilleur, D.A. Myles, A. Podjarny, Eur. Biophys. J. (2006).
[19] D.H. Harrison, K.M. Bohren, G.A. Petsko, D. Ringe, K.H. Gabbay, Biochemistry 36 (1997) 16134–16140.
[20] D.H. Harrison, K.M. Bohren, D. Ringe, G.A. Petsko, K.H. Gabbay, Biochemistry 33 (1994) 2011–2020.
[21] T. Ehrig, K.M. Bohren, F.G. Prendergast, K.H. Gabbay, Biochemistry 33 (1994) 7157–7165.
[22] A. Urzhumtsev, F. Tete-Favier, A. Mitschler, J. Barbanton, P. Barth, L. Urzhumtseva, J.F. Biellmann, A. Podjarny, D. Moras, Structure 5 (1997) 601–612.
[23] K.J. Ruhnau, H.P. Meissner, J.R. Finn, M. Reljanovic, M. Lobisch, K. Schutte, D. Nehrdich, H.J. Tritschler, H. Mehnert, D. Ziegler, Diabet. Med. 16 (1999) 1040–1043.
[24] A.I. Vinik, T.S. Park, K.B. Stansberry, G.L. Pittenger, Diabetologia 43 (2000) 957–973.
[25] C.K. Sen, Biochem. Pharmacol. 55 (1998) 1747–1758.
[26] A.T. Brünger, in: X-PLOR, (Yale University, New Haven, 1993).
[27] G.J. Kleywegt, T.A. Jones, Acta Crystallogr. D. Biol. Crystallogr. 54 (1998) 1119–1131.
[28] T.A. Jones, J.-Y. Zou, S.W. Cowan, M. Kjeldgaard, Acta Crystallogr. A47 (1991) 110–119.
[29] K.J. Ruhnau, H.P. Meissner, J.R. Finn, M. Reljanovic, M. Lobisch, K. Schutte, D. Nehrdich, H.J. Tritschler, H. Mehnert, D. Ziegler, Diabet. Med. 16 (1999) 1040–1043.
[30] K.V. Ramana, B.L. Dixit, S. Srivastava, G.K. Balendiran, S.K. Srivastava, A. Bhatnagar, Biochemistry 39 (2000) 12172–12180.
[31] C.E. Grimshaw, K.M. Bohren, C.J. Lai, K.H. Gabbay, Biochemistry 34 (1995) 14366–14373.
[32] H. Ohtaka, S. Muzammil, A. Schon, A. Velazquez-Campoy, S. Vega, E. Freire, Int. J. Biochem. Cell Biol. 36 (2004) 1787–1799.
[33] A.J. Ruben, Y. Kiso, E. Freire, Chem. Biol. Drug Des. 67 (2006) 2–4.

[34] P. Ou, J. Nourooz-Zadeh, H.J. Tritschler, S. Wolff, Free Radic. Res. 25 (1996) 337–346.
[35] S. Srivastava, B.L. Dixit, K.V. Ramana, A. Chandra, D. Chandra, A. Zacarias, J.M. Petrash, A. Bhatnagar, S.K. Srivastava, Biochem. J. 358 (2001) 111–118.
[36] D.K. Wilson, I. Tarle, J.M. Petrash, F.A. Quiocho, Proc. Natl. Acad. Sci. USA 90 (1993) 9847–9851.
[37] R.A. Engh, R. Huber, Acta Crystallogr A 47 (1998) 392–400.
[38] K.M. Bohren, J.L. Page, R. Shankar, S.P. Henry, K.H. Gabbay, J. Biol. Chem. 266 (1991) 24031–24037.
[39] Z. Otwinowski, W. Minor, Methods in enzymology, in: C.W. Carter Jr., R.M. Sweet (Eds.), Macromolecular Crystallography, part A, vol. 276, Academic Press, New York, 1997, pp. 307–326.
[40] W.L. DeLano, The PyMOL User's Manual, DeLano Scientific, San Carlos, CA, USA, 2002.